

MicroRNA-206 facilitates gastric cancer cell apoptosis and suppresses cisplatin resistance by targeting MAPK2 signaling pathway

Z. CHEN¹, Y.-J. GAO², R.-Z. HOU², D.-Y. DING², D.-F. SONG²,
D.-Y. WANG², Y. FENG²

¹Department of Nephrology, First Hospital of Jilin University, Changchun, Jilin, China

²Department of Gastrointestinal Colorectal and Anal Surgery, China-Japan Union Hospital of Jilin University, Changchun, Jilin, China

Abstract. – OBJECTIVE: Mitogen activating protein kinase 3 (MAPK3) is critical in extracellular signal-regulated kinase (ERK)/MAPK pathway. Gastric cancer tissues have microRNA-206 (miR-206) down-regulation. This study aimed to investigate the role of miR-206 in MAPK3 expression, gastric cancer cell proliferation, apoptosis, and cisplatin (DDP) resistance.

MATERIALS AND METHODS: Dual-Luciferase reporter gene assay confirmed targeted regulation between miR-206 and MAPK3. DDP resistant cell line BGC823/DDP and SGC7901/DDP were generated for comparing miR-206 and MAPK3 expression against parental cells using quantitative Real Time-Polymerase Chain Reaction (qRT-PCR) and Western blot, followed by flow cytometry measuring apoptosis. Drug-resistant cells were transfected with miR-206 mimic for measuring MAPK3 and phosphorylated MAPK3 (p-MAPK3) expression. Flow cytometry and EdU were employed for measuring cell apoptosis and proliferation.

RESULTS: Targeted regulation existed between miR-206 and MAPK3 mRNA. BGC823/DDP and SGC7901/DDP cell presented lower miR-206 than parental cells, plus higher MAPK3 mRNA or protein. Under DDP treatment equivalent to IC50 of parental cells, drug-resistant cells presented lower apoptosis compared to parental drug-sensitive cells. Compared to miR-normal control (miR-NC) group, miR-206 mimic transfection significantly decreased MAPK3 and p-MAPK3 protein expression ($p < 0.05$), enhanced cell apoptosis and weakened proliferation potency ($p < 0.05$).

CONCLUSIONS: The down-regulation of miR-206 is associated with DDP resistance of gastric cancer cells. Up-regulating miR-206 expression can weaken the proliferation of drug-resistant gastric cancer cells, facilitate cell apoptosis and decrease DDP resistance via targeted inhibition of MAPK3 expression.

Key Words:

Gastric cancer, DDP, Drug resistance, MiR-206, MAPK3.

Introduction

Gastric cancer (GC) is a commonly occurred malignant tumor in the digestive tract in clinics. It is the fourth common malignant tumor and second deadly cancer, only lower than the most deadly lung cancer^{1,2}. Chemotherapy is crucial for GC treatment, but drug resistance largely restricts efficiency, and affects patient survival or prognosis^{3,4}.

Mitogen-activated protein kinase 3 (MAPK3), or extracellular signal-regulated kinase 1 (ERK1) is an important signal transduction molecule in the ERK/MAPK pathway, and plays crucial roles in activating the ERK/MAPK pathway for transducing downstream signals^{5,6}. Previous studies⁷⁻⁹ showed the role of functional enhancement of MAPK3 in the onset and progression of GC. MicroRNA (miR) is one type of endogenous non-coding small RNA molecules in eukaryotes, and can mediate the target gene expression via complementary binding to 3'-untranslated region (3'-UTR) of target gene mRNA to degrade mRNA or inhibit mRNA translation. Therefore, miR could modulate the biological processes, including cell survival, proliferation, apoptosis and migration. The role of abnormal expression or function of miR in tumor drug resistance is drawing lots of research interests^{10,11}. MiR-206 is a miR molecule with relatively more studies, and can mediate drug resistance of lung cancer and colon cancer cells^{12,13}. Researchers¹⁴⁻¹⁶ showed

the relationship between abnormal expression of miR-206 and occurrence, metastasis and prognosis of GC, but with fewer studies regarding GC drug resistance. Bioinformatics analysis showed the existence of targeted complementary binding sites between miR-206 and 3'-UTR of MAPK3 mRNA, suggesting potentially targeted regulation. This study thus investigated if miR-206 played a role in modulating MAPK3 expression, affecting the ERK/MAPK pathway activity and DDP resistance of GC cells.

Materials and Methods

Major Reagent and Materials

Normal gastric mucosal epithelial cell RGM-1 and GC cell lines BGC823 and SGC7901 were purchased from Junrui Biotechnology (Shanghai, China). HEK293T cells were purchased from Shanghai Cell Bank, Chinese Academy of Sciences (Shanghai, China). Roswell Park Memorial Institute-1640 (RPMI-1640), option minimal essential medium (Opti-MEM) and fetal bovine serum (FBS) were purchased from Gibco Co. Ltd. (Grand Island, NY, USA). TRIzol and Lipofectamine 2000 transfection reagent were purchased from Invitrogen (Carlsbad, CA, USA). QuantiTect SYBR Green RT-PCR kit was purchased from Qiagen (Hilden, Germany). MiR-206 mimic and miR-NC were purchased from RioBio Ltd. (Guangzhou, China). Rabbit anti-human MAPK3 and p-MAPK3 polyclonal antibody were purchased from Santa Cruz Biotechnology (Santa Cruz, CA, USA). Rabbit anti-human β -actin was purchased from Cell Signaling Technology (Danvers, MA, USA). Goat anti-rabbit horseradish peroxidase (HRP) conjugated secondary antibody was purchased from Jackson ImmunoResearch (West Grove, PA, USA). Annexin V-FITC/PI Apoptosis Detection Kit was purchased from Yusheng Biotechnology (Shanghai, China). BeyoECL Plus chemiluminescent reagent and bicinchoninic acid (BCA) protein quantification kit were purchased from Beyotime Biotechnology (Shanghai, China). EdU Flow Cytometry Kit and cisplatin (DDP) were purchased from Sigma-Aldrich (St. Louis, MO, USA). Cell Counting Kit-8 (CCK-8) was purchased from Dojindo Molecular Technologies (Kumamoto, Japan). Luciferase activity assay kit Dual-Glo Luciferase Assay System and pMIR plasmid were purchased from Promega (Madison, WI, USA).

Cell Culture

BGC823 and SGC7901 cells were kept in RPMI-1640 medium containing 10% FBS, and were incubated in a 37°C chamber (Model: HERAcell 240i, Thermo Fisher Scientific, Waltham, MA, USA) with 5% CO₂. RGM-1 cells were kept in Dulbecco's Modified Eagle Medium (DMEM)/F12 medium containing 10% FBS, in a 37°C chamber with 5% CO₂. Cells were passed at 1:4 ratio. Those cells at log-growth phase were used for experiments. This study was approved by the Ethics Committee of the First Hospital of Jilin University, Changchun, Jilin, China.

Generation of DDP Resistant Cell Model

For generating DDP resistant cell model, BGC823 and SGC7901 cells at log-growth phase were supplemented with DDP at 0.1 μ g/ml final concentration. After stable growth for 2 weeks, DDP concentration was gradually elevated to 0.2 μ g/ml for 2 weeks incubation. Following similar procedures, DDP treatment concentration was gradually increased to 0.4 μ g/ml and 0.8 μ g/ml until BGC823 and SGC7901 cells can maintain stable growth and repeated passage within 0.8 μ g/ml, thus generating DDP resistant GC cell lines BGC823/DDP and SGC7901/DDP.

BGC823, SGC7901, BGC823/DDP and SGC7901/DDP cells were seeded into 96-well plate at 10000 cells per well density. After 24 h attached growth, cells were treated with 0, 0.1, 1, 10, 100 and 1000 μ g/ml DDP, with 6 replicated samples were set for each concentration. After 48 h of incubation, 10 μ l CCK-8 solution was added into each well. Absorbance (A) values at 450 nm wavelength (A₄₅₀) of each well were measured after 4 h reaction. Inhibition rate = $(1 - A_{450} \text{ of drug treatment group}) / A_{450} \text{ of control group} \times 100\%$. SPSS software was used to calculate the drug concentration for achieving half-inhibition rate for cell growth (IC₅₀). Resistance index (RI) = IC₅₀ of drug-resistant cells / IC₅₀ of parental cells.

Flow Cytometry for Cell Proliferation

EdU Flow Cytometry Kit was used to measure cell proliferation. In brief, cultured cells were re-suspended in RPMI-1640 medium containing 10% FBS and were incubated in 10 μ M EdU at 37°C for 2 h. Cells were then seeded into culture plate for 48 h incubation and were digested by trypsin for collection. After centrifugation and rinsing in Phosphate-Buffered Saline (PBS), cells were fixed in paraformaldehyde and permeabilized in 100 μ l buffer. 500 μ l reaction buffer was

added for 30 min dark incubation at room temperature. Total of 3 ml permeabilization buffer was then added one time for centrifugation and rinsing. Total of 500 μ l wash buffer was added for re-suspending cells, and cell proliferation was measured using FC500MCL flow cytometry (Beckman Coulter Inc., Fullerton, CA, USA).

Dual-Luciferase Activity Assay

PCR products for full length or mutant form of 3'-UTR of MAPK3 gene were digested by dual restriction enzymes for connecting to pMIR plasmid. After bacterial transfection, sequencing was performed to screen plasmids with correct sequence and was named as pMIR-MAPK3-WT and pMIR-MAPK3-MUT. Lipofectamine 2000 was used to co-transfect pMIR-MAPK3-WT (or pMIR-MAPK3-MUT) and miR-206 (or miR-NC) into HEK293T cells. Cells were kept in a 37°C chamber with 5% CO₂ for 48 h of incubation. Dual-Glo Luciferase Assay System was used to measure the activity of Dual-Luciferase.

Cell Transfection and Grouping

Cultured BGC823/DDP and SGC7901/DDP cells were divided into two groups: miR-NC transfection group and miR-206 mimic transfection group. In brief, 100 μ l serum-free Opti-MEM was used to dilute 10 μ l Lipofectamine 2000, 50 nmol miR-NC, 50 nmol miR-206 mimics. After 5 min room temperature incubation, Lipofectamine 2000 was gently mixed with miR-NC and miR-206 mimic for 20 min room temperature incubation. The transfection mixture was added into RPMI-1640 medium containing 10% FBS. After 72 h of gentle incubation, cells were collected.

Cells from all treatment groups were seeded into 6-well plate. When reaching 50% confluences, 0.8 μ g/ml DDP was added for 48 h continuous incubation. Apoptosis was measured by flow cytometry as described in the following methods.

Cells from all treatment groups were digested by trypsin and collected. After 2 h of incubation in 10 μ M EdU, cells were continuously incubated for 48 h as described in previous sections. EdU positive rate was measured by EdU Flow Cytometry Kit to reflect cell proliferation potency.

Quantitative Real Time-PCR (qRT-PCR) for Gene Expression

TRIzol was used to extract cellular RNA. One-step qRT-PCR was used to measure gene expression using QuantiTect SYBR Green RT-PCR kit (Cat. No. 204243, Qiagen, Hilden, Germany). In

a 20 μ l qRT-PCR reaction system, one added 10.0 μ l 2 \times QuantiTect SYBR Green RT-PCR Master Mix, 1.0 μ l forward and reverse primer (0.5 μ M/l), 2 μ g template RNA, 0.5 μ l QuantiTect RT Mix, and ddH₂O. qRT-PCR conditions were: 45°C 5 min and 94°C 30 s, followed by 40 cycles each consisting of 95°C 5 s and 60°C 30 s. The gene expression was measured on Bio-Rad CFX96 Real Time-fluorescent quantitative PCR cycler (Bio-Rad Laboratories, Hercules, CA, USA).

Western Blot

100 μ l radioimmunoprecipitation assay lysis buffer (RIPA) was added into each 1 \times 10⁶ cells to extract proteins, whose concentration was determined by the BCA approach. 40 μ g protein samples was loaded onto sodium dodecyl sulfate-polyacrylamide gel electrophoresis (SDS-PAGE) (10% separating gel and 4% condensing gel) for separation (45 V, 150 min), and was transferred to polyvinylidene difluoride (PVDF) membrane (250 mA, 100 min). The membrane was blocked in 5% defatted milk powder and was incubated in primary antibody (MAPK3 at 1:2000, p-MAPK3 at 1:1000, β -actin at 1:10000) at 4°C overnight. On the next day, the membrane was rinsed in PBS-Tween-20 (PBST) three times, and HRP conjugated secondary antibody (1:15000 dilution) was used for 60 min incubation. After three times of PBST rinsing, an equal volume of BeyoECL Plus working solution A and B were mixed and applied onto the protein blotting membrane. After dark incubation for 2-3 min, the membrane was exposed and the X-ray film was scanned for data storage.

Cell Apoptosis Assay

The cells were digested in trypsin and collected, followed by centrifugation for washing. Cells were resuspended in 100 μ l Annexin V Binding Buffer, 10 μ l Annexin V-fluorescein isothiocyanate (FITC) and 5 μ l propidium iodide (PI) were sequentially added for 15 min room temperature incubation. 400 μ l Annexin V Binding Buffer was added for measuring cell apoptosis on FC500 MCL flow cytometry (Beckman Coulter Inc., Fullerton, CA, USA).

Statistical Analysis

SPSS 18.0 software was used for data analysis (SPSS Inc., Chicago, IL, USA). Measurement data were presented as mean \pm standard deviation (SD). The Student's *t*-test was used for comparing measurement data between the two groups. The com-

parison among multiple groups was performed by one-way analysis variance (ANOVA) first, followed by Bonferroni post-hoc comparison. A statistical significance was identified when $p < 0.05$.

Results

Targeted Regulation Between MiR-206 and MAPK3 mRNA

Bioinformatics analysis showed the existence of complementary binding sites between miR-206 and 3'-UTR of MAPK3 mRNA (Figure 1A). Dual-Luciferase activity reporter assay showed that transfection of miR-206 mimic remarkably depressed the relative Luciferase activity in HEK293T cells transfected with pMIR-MAPK3-WT, but did not affect the relative Luciferase activity in HEK293T cells transfected with a pMIR-MAPK3-MUT plasmid (Figure 1B). These results suggest that miR-206 could target on 3'-UTR of MAPK3 mRNA for suppressing its expression.

Drug-Resistant Tumor Cells Presented Strong Apoptotic Resistance

BGC823 cells had IC_{50} value of 0.57 ± 0.06 $\mu\text{g/ml}$, whilst drug-resistant cell BGC823/DDP

had IC_{50} at 5.26 ± 0.72 $\mu\text{g/ml}$. As a result, BGC823/DDP cells had RI of 9.23 (Figure 2A). In similar, SGC7901 cells had IC_{50} value at 1.17 ± 0.14 $\mu\text{g/ml}$, and SGC7901/DDP cells had IC_{50} value as high as 14.73 ± 1.56 $\mu\text{g/ml}$, making the RI of SGC7901/DDP cells at 12.59 (Figure 2B).

Under the treatment of 0.57 $\mu\text{g/ml}$ DDP, BGC823 cells had relatively higher apoptotic rate, reaching $31.6\% \pm 3.2\%$, and BGC823/DDP cells had apoptotic rate at only $4.2\% \pm 0.7\%$ (Figure 2C). Under 1.17 $\mu\text{g/ml}$ DDP treatment, SGC7901 cells had apoptotic rate as high as $22.6\% \pm 2.5\%$, whilst SGC7901/DDP cells had apoptotic rate at only $3.3\% \pm 0.6\%$ (Figure 2D).

Downregulation of MiR-206 and Upregulation of MAPK3 in Drug-Resistant Cells

The qRT-PCR results showed that, compared to RGM-1 cells, BGC823 and BGC823/DDP cells had remarkably decreased miR-206 expression, with a lower level in drug-resistant cells. In similar patterns, SGC7901/DDP cells had remarkably lower miR-206 expression than SGC7901 cells, which showed lower miR-206 level than RGM-1 cells (Figure 3A). Compared to RGM-1 cells, BGC823 cells had remarkably elevated MAPK3 mRNA, and BGC823/DDP cells had further higher MAPK3 mRNA expression than BGC823 cells. SGC7901/DDP cells also showed significantly higher MAPK3 mRNA level than SGC7901 cells, which showed significantly higher MAPK3 mRNA than RGM-1 cells (Figure 3B). Western blot analysis showed that, compared to RGM-1 cells, BGC823 cells had markedly elevated MAPK3 protein expression, and BGC823/DDP cells had further higher MAPK3 protein level than BGC823 cells. For SGC7901/DDP cells, they also had higher MAPK3 protein level than SGC7901 cells, which had higher MAPK3 protein level than RGM-1 cells (Figure 3C).

Overexpression of MiR-206 Decreased DDP Resistance of GC Cells

The qRT-PCR results showed that, compared to miR-NC transfection, miR-206 mimic remarkably down-regulated MAPK3 mRNA expression in BGC823/DDP and SGC7901/DDP cells (Figure 4A). Western blot results further showed that, compared to miR-NC group, the miR-195 mimic transfection remarkably suppressed MAPK3 and p-MAPK3 protein expression in BGC823/DDP

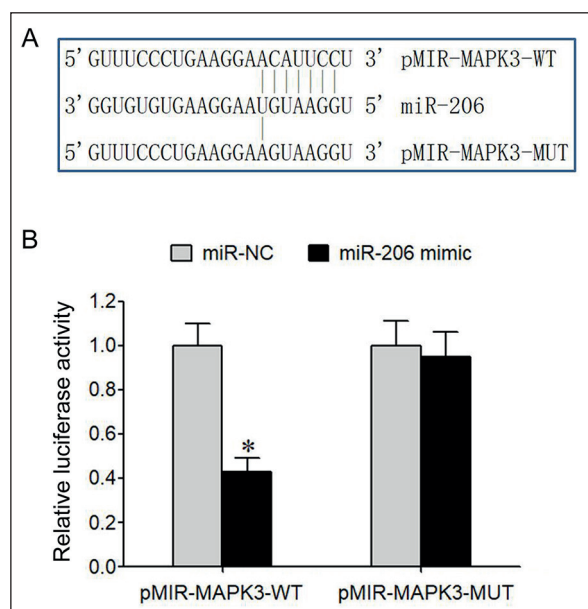


Figure 1. Targeted regulation between miR-206 and MAPK3 mRNA. **A**, Schematic diagram for functional site between miR-206 and 3'-UTR of MAPK3 mRNA. **B**, Dual-Luciferase gene reporter assay. * $p < 0.05$ compared to the miR-NC group.

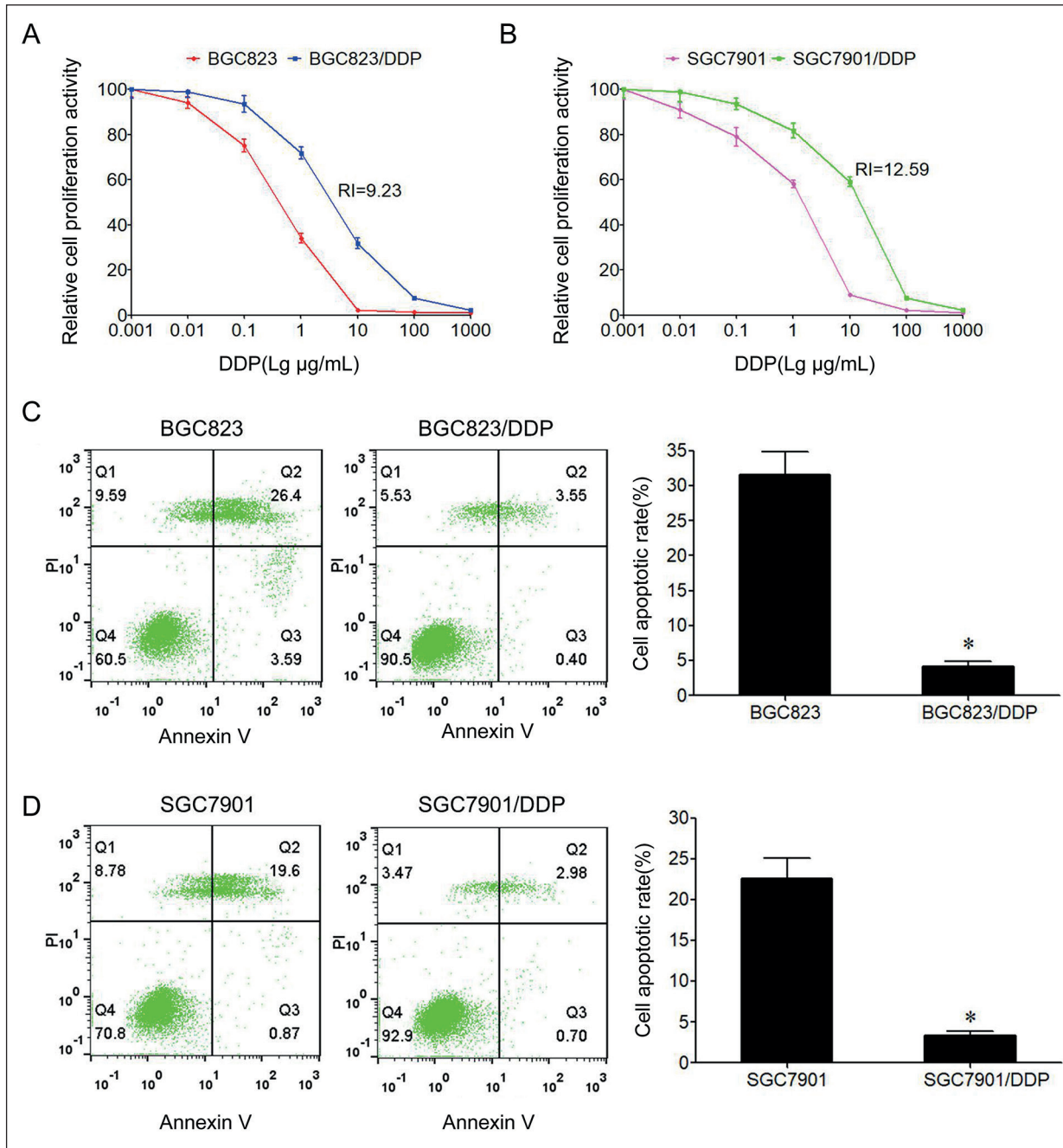


Figure 2. Drug-resistant cells present strong apoptotic resistance. **A**, CCK-8 assay for proliferation activity of BGC823 and BGC823/DDP cells. **B**, CCK-8 assay for proliferation activity of SGC7901 and SGC7901/DDP cells. **C**, Flow cytometry for apoptosis of BGC823 and BGC823/DDP cells. **D**, Flow cytometry for apoptosis of SGC7901 and SGC7901/DDP cells. * $p < 0.05$ comparing the two groups.

and SGC7901/DDP cells (Figure 4B). Flow cytometry results showed that transfection of miR-195 mimic significantly elevated apoptosis of BGC823/DDP and SGC7901/DDP cells (Figure 4C, $p < 0.05$), whilst cell proliferation potency was markedly inhibited (Figure 4D).

Discussion

Both incidence and mortality of GC are among the top rolls of systemic malignant tumors. It is estimated that more than 1.3 million people are newly diagnosed as GC¹⁷. Having the highest GC

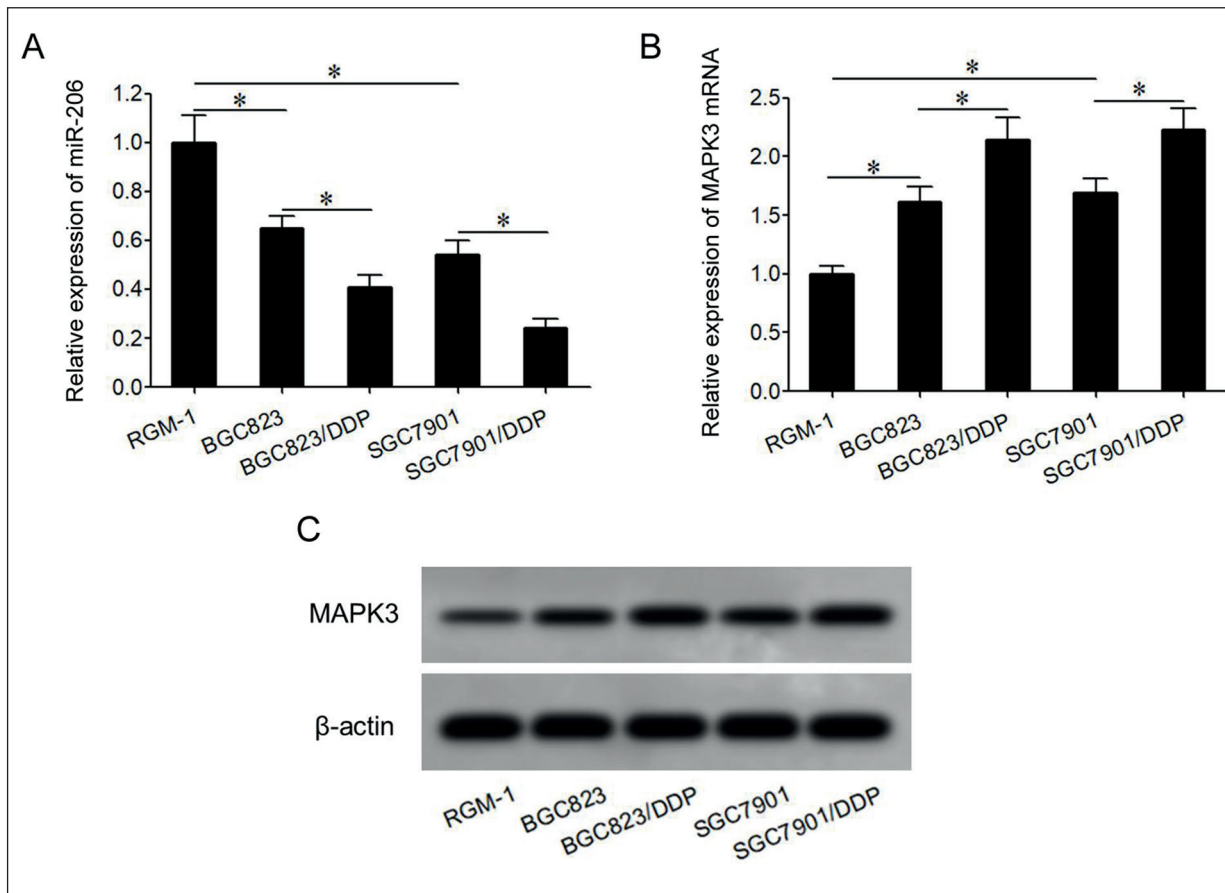


Figure 3. Down-regulation of miR-206 and up-regulation of MAPK3 in drug-resistant cells. **A**, qRT-PCR for measuring miR-206 expression. **B**, qRT-PCR for measuring MAPK3 mRNA expression. **C**, Western blot for MAPK3 protein expression quantification. * $p < 0.05$ comparing the two groups.

incidence, almost one half of GC occurred in China¹⁸. Chemotherapy is a critical measure for GC treatment. However, the individual patient had large variations of chemotherapy sensitivity, making drug resistance an important factor restricting GC chemotherapy efficiency and affecting patient survival or prognosis^{3,4}.

Four major signal transduction pathways exist in the MAPK signaling pathways, including ERK, c-Jun N-terminal kinase (JNK), p38 MAPK and ERK5/big MAP kinase 1 (BMK1). Among those ERK-induced MAPK transduction is the classical MAPK signaling pathway, and the major transduction route by which the MAPK signaling pathway exerts its major effects¹⁹⁻²¹. The ERK/MAPK signal transduction pathway is widely distributed in various tissues and cells, and can regulate various biological processes including cell proliferation, apoptosis and invasion²²⁻²⁵, and is closely correlated with tumor pathogenesis, progression and drug resistance²⁶⁻²⁸. MAPK

is a serine/threonine kinase, and can modulate nuclear translocation of cytosolic proteins by phosphorylation after receiving upstream cascade reaction, thus modulating functions of nuclear transcription factors such as C-fos or C-Jun by phosphorylation, mediating cell proliferation and apoptosis²⁹⁻³⁰. Enhanced expression and functional activity play important roles in the onset, progression, metastasis and drug resistance of various tumors including ovarian cancer, lung cancer and breast cancer³¹⁻³⁴. Scholars⁷⁻⁹ have shown the critical role of enhanced MAPK3 functional activity in the onset and progression of GC. Moreover, abnormal expression of miR-206 is correlated with GC pathogenesis, metastasis and prognosis¹⁴⁻¹⁶. However, few studies have been performed regarding the relationship between miR-206 and GC drug resistance. Bioinformatics analysis found the existence of complementary binding sites between miR-206 and 3'-UTR of MAPK3 mRNA, indicating possibly regulatory

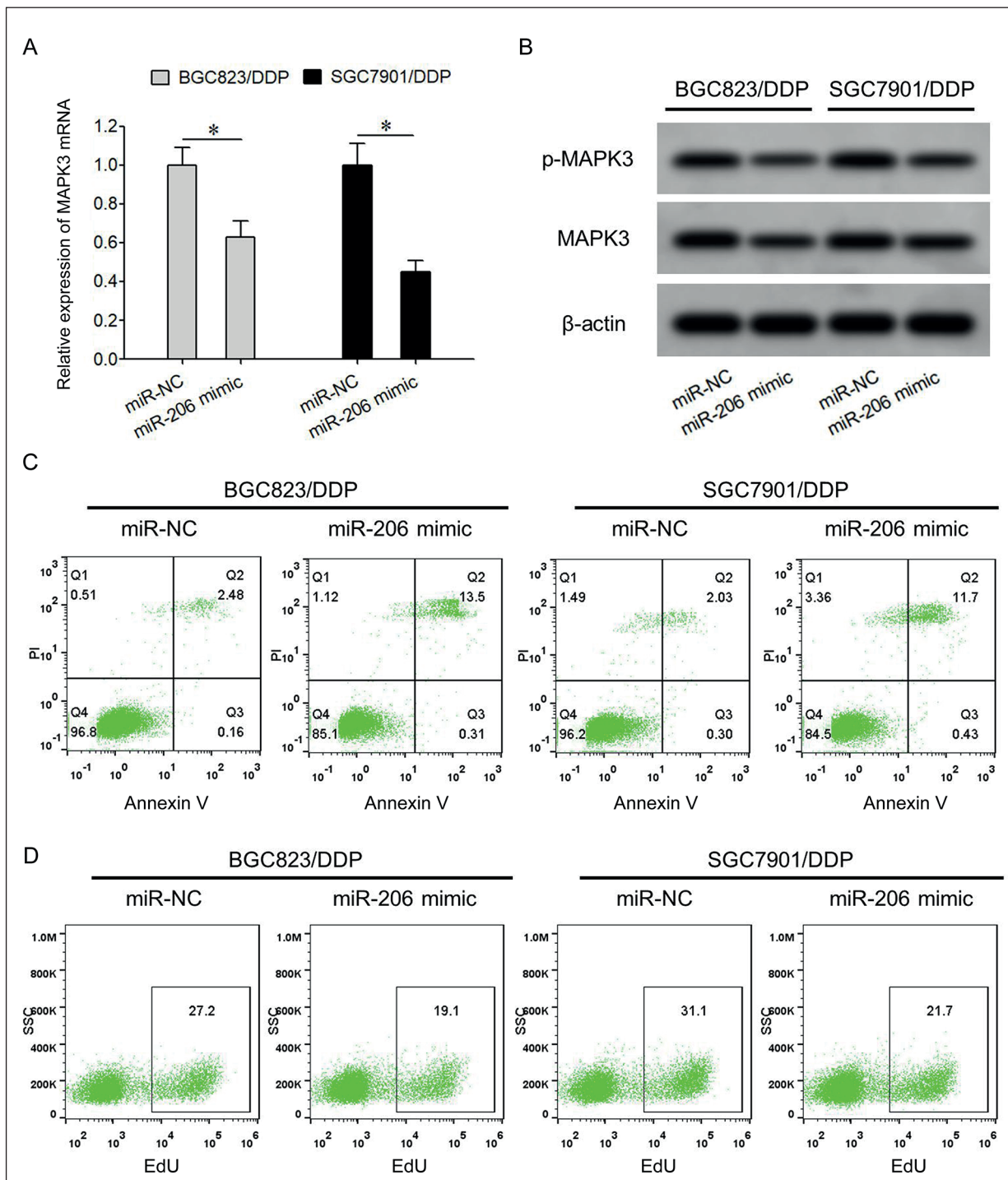


Figure 4. Over-expression of miR-206 suppressed DDP resistance of GC cells. **A**, qRT-PCR for MAPK3 mRNA expression. **B**, Western blot for protein expression. **C**, Flow cytometry for cell apoptosis. **D**, Flow cytometry for cell proliferation. * $p < 0.05$ comparing the two groups.

functions. This work investigated if miR-206 played a role in modulating MAPK3 expression, affecting pathway activity of ERK/MAPK and DDP resistance of GC cells.

Dual-Luciferase gene reporter assay showed that transfection of miR-206 mimic significantly depressed the relative Luciferase activity in HEK293T cells transfection with pMIR-MAPK3-

WT, but did not affect the relative Luciferase activity in HEK293T cells transfecting with pMIR-MAPK3-MUT, indicating targeted regulation between miR-206 and MAPK3 mRNA. Based on the CCK-8 assay, we calculated IC_{50} against DDP of both parental and drug-resistant cells. The results showed that IC_{50} of drug-resistant cells BGC823/DDP and SGC7901/DDP were all significantly higher than parental BGC823 and SG7901 cells, obtaining RI of BGC823/DDP and SGC7901/DDP at 9.23 and 12.59, respectively. Flow cytometry for apoptotic assay showed prominent apoptotic resistance of BGC823/DDP and SGC7901/DDP cells, suggesting a successful generation of DDP resistant GC cells satisfying further experiments. Both gene and protein assays showed that, compared to normal gastric mucosal cells, GC cells presented significantly decreased miR-206 expression, whilst DDP resistant GC cells had even lower miR-206 expression. GC cells showed markedly higher MAPK3 mRNA and protein expression than normal gastric mucosal epithelium, whilst drug-resistant cell line had even higher MAPK3 mRNA and protein expression. The results suggested the role of miR-206 down-regulation in enhancing MAPK3 expression, as it is not only related to GC pathogenesis, but also participates in the regulation of GC drug resistance. Ren et al¹⁵ found that, compared to normal tissues, GC tissues presented remarkably lower miR-206 expression by 75%, and miR-206 expression was related to primary infiltration, distal metastasis and TNM stage of GC. Compared to normal gastric mucosal cell line GES-1, GC cell lines SGC-7901, BGC-823 and AGS all presented remarkably lower miR-206 expression. Shi et al¹⁴ found that, compared to tumor-adjacent tissues, GC patients presented remarkably decreased miR-206 expression, and its expression level was correlated with tumor infiltration depth, lymph node metastasis and TNM stage. Moreover, miR-206 expression was related to patient survival and prognosis, as those patients with relatively lower miR-206 expression had a significantly lower survival rate compared to those with miR-206 over-expression. Yang et al¹⁶ also found that miR-206 expression level in GC tumor tissues was related to lymph node metastasis, venous metastasis, disease stage and recurrence, plus the value of miR-206 expression as an independent predictive factor for patient survival and prognosis. Zhang et al³⁵ showed significant decreased of miR-206 in GC tumor tissues and cell lines. Zhang et al³⁶ further found

remarkably decreased miR-206 expression in GC cell lines, and those cells with high metastasis potency including SGC7901-M and MKN29-M had even lower miR-206 expression compared to low-metastatic cell lines such as SGC7901-NM and MKN28-NM. Zheng et al³⁷ also found that, compared to tumor-adjacent tissues, GC tissues had markedly decreased miR-206 expression. All these results demonstrated the tumor suppressor role of miR-206 in GC and the correlation between miR-206 down-regulation with GC, similar to our observations.

However, the relationship between miR-206 and GC drug resistance is not clear yet. This study further investigated if miR-206 played a role in modulating GC cell drug resistance. The results showed that transfection of miR-206 mimic can markedly depressed MAPK3 protein expression in BGC823/DDP and SGC7901/DDP cells, enhancing the apoptosis of BGC823/DDP and SGC7901/DDP cells that can maintain stable growth in DDP, plus remarkable inhibition of cell proliferation, and decreased drug resistance. Zhang et al³⁶ found that miR-206 could inhibit migration or invasion of cultured GC cell MKN28-M and weaken its growth and metastatic ability in BALB/c nude mice via targeted inhibition on PAX3 expression. Ren et al¹⁵ found that the over-expression of miR-206 can inhibit the proliferation of GC cell line SGC7901, induce cell cycle arrest, weaken *in vitro* migration or invasion potency of SGC7901 cells and inhibit its distal metastasis in the animal model by modulating the expression of tumor metastasis-related genes STC2, HDAC4 and KLF4. Zhang et al³⁵ showed the targeted regulation between miR-206 and CCND2, and the over-expression of miR-206 can weaken proliferation and clonal formation potency of GC cells by suppressing CCND2 expression, and inducing cell cycle arrest at the G0/G1 phase. Zheng et al³⁷ found that the up-regulation of miR-206 remarkably suppressed c-Met expression in GC cells AGS, inhibit its migration or invasion, induce cell cycle arrest at G1 phase and decrease its tumorigenesis potency in nude mice. All these findings demonstrated the role of miR-206 in alleviating malignant biological properties of GC cells, as similar with our observations. In contrast to these studies, our results revealed the role of miR-206 in suppressing DDP drug resistance of GC cells via targeted inhibition on MAPK3 expression, which has not been previously described. However, whether the regulation of MAPK3 expression by miR-206 is related to

drug resistance of GC patients is still unclear. Further investigations are required to detect the differential expression of miR-206 and MAPK3 in tumor tissues between chemotherapy sensitive and resistant patients, to satisfy the weakness of this study.

Conclusions

We found that miR-206 down-regulation is correlated with DDP resistance of GC cells. The up-regulation of miR-206 can weaken proliferation potency of GC via targeted inhibition on MAPK3 expression, thus facilitating cell apoptosis and decreasing its DDP resistance.

Conflict of Interest

The Authors declare that they have no conflict of interests.

Acknowledgements

This work was supported by the Scientific and Technological Development Project of Jilin Province of China (No. 20160101115JC and No. 20180519025JH).

References

- LI LO, PAN D, ZHANG SW, Y XIE D, ZHENG XL, CHEN H. Autophagy regulates chemoresistance of gastric cancer stem cells via the Notch signaling pathway. *Eur Rev Med Pharmacol Sci* 2018; 22: 3402-3407.
- ANG TL, FOCK KM. Clinical epidemiology of gastric cancer. *Singapore Med J* 2014; 55: 621-628.
- MARIN JJ, AL-ABDULLA R, LOZANO E, BRIZ O, BUJANDA L, BANALES JM, MACIAS RI. Mechanisms of resistance to chemotherapy in gastric cancer. *Anticancer Agents Med Chem* 2016; 16: 318-334.
- YU P, DU Y, YANG L, FAN S, WU J, ZHENG S. Significance of multidrug resistance gene-related proteins in the postoperative chemotherapy of gastric cancer. *Int J Clin Exp Pathol* 2014; 7: 7945-7950.
- JIN E, HAN S, SON M, KIM SW. Cordyceps bassiana inhibits smooth muscle cell proliferation via the ERK1/2 MAPK signaling pathway. *Cell Mol Biol Lett* 2016; 21: 24.
- BARGAGNA-MOHAN P, ISHII A, LEI L, SHEEHY D, PANDIT S, CHAN G, BANSAL R, MOHAN R. Sustained activation of ERK1/2 MAPK in Schwann cells causes corneal neurofibroma. *J Neurosci Res* 2017; 95: 1712-1729.
- WANG X, YU Z, ZHOU Q, WU X, CHEN X, LI J, ZHU Z, LIU B, SU L. Tissue transglutaminase-2 promotes gastric cancer progression via the ERK1/2 pathway. *Oncotarget* 2016; 7: 7066-7079.
- GAO P, WANG S, JING F, ZHAN J, WANG Y. microRNA-203 suppresses invasion of gastric cancer cells by targeting ERK1/2/Slug/ E-cadherin signaling. *Cancer Biomark* 2017; 19: 11-20.
- LI PY, LV J, QI WW, ZHAO SF, SUN LB, LIU N, SHENG J, QIU WS. Tspan9 inhibits the proliferation, migration and invasion of human gastric cancer SGC7901 cells via the ERK1/2 pathway. *Oncol Rep* 2016; 36: 448-454.
- ARMSTRONG CM, LIU C, LOU W, LOMBARD AP, EVANS CP, GAO AC. MicroRNA-181a promotes docetaxel resistance in prostate cancer cells. *Prostate* 2017; 77: 1020-1028.
- LI F, MAHATO RI. MicroRNAs and drug resistance in prostate cancers. *Mol Pharm* 2014; 11: 2539-2552.
- JIAO D, CHEN J, LI Y, TANG X, WANG J, XU W, SONG J, LI Y, TAO H, CHEN Q. miR-1-3p and miR-206 sensitizes HGF-induced gefitinib-resistant human lung cancer cells through inhibition of c-Met signaling and EMT. *J Cell Mol Med* 2018; 22: 3526-3536.
- MENG X, FU R. miR-206 regulates 5-FU resistance by targeting Bcl-2 in colon cancer cells. *Onco Targets Ther* 2018; 11: 1757-1765.
- SHI H, HAN J, YUE S, ZHANG T, ZHU W, ZHANG D. Prognostic significance of combined microRNA-206 and CyclinD2 in gastric cancer patients after curative surgery: a retrospective cohort study. *Biomed Pharmacother* 2015; 71: 210-215.
- REN J, HUANG HJ, GONG Y, YUE S, TANG LM, CHENG SY. MicroRNA-206 suppresses gastric cancer cell growth and metastasis. *Cell Biosci* 2014; 4: 26.
- YANG Q, ZHANG C, HUANG B, LI H, ZHANG R, HUANG Y, WANG J. Downregulation of microRNA-206 is a potent prognostic marker for patients with gastric cancer. *Eur J Gastroenterol Hepatol* 2013; 25: 953-957.
- GUGGENHEIM DE, SHAH MA. Gastric cancer epidemiology and risk factors. *J Surg Oncol* 2013; 107: 230-236.
- LAN H, ZHU N, LAN Y, JIN K, TENG L. Laparoscopic gastrectomy for gastric cancer in China: an overview. *Hepatogastroenterology* 2015; 62: 234-239.
- WANG DW, WANG YQ, SHU HS. MiR-16 inhibits pituitary adenoma cell proliferation via the suppression of ERK/MAPK signal pathway. *Eur Rev Med Pharmacol Sci* 2018; 22: 1241-1248.
- LI B, LIU YH, SUN AG, HUAN LC, LI HD, LIU DM. MiR-130b functions as a tumor promoter in glioma via regulation of ERK/MAPK pathway. *Eur Rev Med Pharmacol Sci* 2017; 21: 2840-2846.
- BUCHEGGER K, SILVA R, LOPEZ J, ILI C, ARAYA JC, LEAL P, BREBI P, RIQUELME I, ROA JC. The ERK/MAPK pathway is overexpressed and activated in gallbladder cancer. *Pathol Res Pract* 2017; 213: 476-482.
- ZHANG G, CHENG Y, ZHANG Q, LI X, ZHOU J, WANG J, WEI L. ATXLPA axis facilitates estrogen-induced endometrial cancer cell proliferation via MAPK/ERK signaling pathway. *Mol Med Rep* 2018; 17: 4245-4252.

- 23) LIAO T, WEN D, MA B, HU JQ, OU N, SHI RL, LIU L, GUAN Q, LI DS, JI QH. Yes-associated protein 1 promotes papillary thyroid cancer cell proliferation by activating the ERK/MAPK signaling pathway. *Oncotarget* 2017; 8: 11719-11728.
- 24) LU Y, LI Y, XIANG M, ZHOU J, CHEN J. Khat promotes human breast cancer MDA-MB-231 cell apoptosis via mitochondria and MAPK-associated pathways. *Oncol Lett* 2017; 14: 3947-3952.
- 25) YANG XL, LIU KY, LIN FJ, SHI HM, OU ZL. CCL28 promotes breast cancer growth and metastasis through MAPK-mediated cellular anti-apoptosis and pro-metastasis. *Oncol Rep* 2017; 38: 1393-1401.
- 26) JIAO S, WANG SY, HUANG Y. LncRNA PRNCR1 promoted the progression of eclampsia by regulating the MAPK signal pathway. *Eur Rev Med Pharmacol Sci* 2018; 22: 3635-3642.
- 27) MCGIVERN N, EL-HELALI A, MULLAN P, MCNEISH IA, PAUL HARKIN D, KENNEDY RD, MCCABE N. Activation of MAPK signalling results in resistance to sunitinib (AZD0530) in ovarian cancer. *Oncotarget* 2018; 9: 4722-4736.
- 28) HEW KE, MILLER PC, EL-ASHRY D, SUN J, BESSER AH, INCE TA, GU M, WEI Z, ZHANG G, BRAFFORD P. MAPK activation predicts poor outcome and the MEK inhibitor, selumetinib, reverses antiestrogen resistance in ER-positive high-grade serous ovarian cancer. *Clin Cancer Res* 2016; 22: 935-947.
- 29) XIAO P, LIU XW, ZHAO NN, FANG R, WEN Q, ZENG KX, WANG YL. Correlations of neuronal apoptosis with expressions of c-Fos and c-Jun in rats with post-ischemic reconditioning damage. *Eur Rev Med Pharmacol Sci* 2018; 22: 2832-2838.
- 30) MCGINNIS LA, LEE HJ, ROBINSON DN, EVANS JP. MAPK3/1 (ERK1/2) and myosin light chain kinase in mammalian eggs affect myosin-II function and regulate the metaphase II state in a calcium- and zinc-dependent manner. *Biol Rep* 2015; 92: 146.
- 31) KIELBIK M, KRZYZANOWSKI D, PAWLIK B, KLINK M. Cisplatin-induced ERK1/2 activity promotes G1 to S phase progression which leads to chemoresistance of ovarian cancer cells. *Oncotarget* 2018; 9: 19847-19860.
- 32) LI B, LIU YH, SUN AG, HUAN LC, LI HD, LIU DM. MiR-130b functions as a tumor promoter in glioma via regulation of ERK/MAPK pathway. *Eur Rev Med Pharmacol Sci* 2018; 22: 2840-2846.
- 33) DOU H, YAN Z, ZHANG M, XU X. APRIL promotes non-small cell lung cancer growth and metastasis by targeting ERK1/2 signaling. *Oncotarget* 2017; 8: 109289-109300.
- 34) HO JY, HSU RJ, WU CH, LIAO GS, GAO HW, WANG TH, YU CP. Reduced miR-550a-3p leads to breast cancer initiation, growth, and metastasis by increasing levels of ERK1 and 2. *Oncotarget* 2016; 7: 53853-53868.
- 35) ZHANG L, LIU X, JIN H, GUO X, XIA L, CHEN Z, BAI M, LIU J, SHANG X, WU K, PAN Y, FAN D. miR-206 inhibits gastric cancer proliferation in part by repressing cyclinD2. *Cancer Lett* 2013; 332: 94-101.
- 36) ZHANG L, XIA L, ZHAO L, CHEN Z, SHANG X, XIN J, LIU M, GUO X, WU K, PAN Y, FAN D. Activation of PAX3-MET pathways due to miR-206 loss promotes gastric cancer metastasis. *Carcinogenesis* 2015; 36: 390-399.
- 37) ZHENG Z, YAN D, CHEN X, HUANG H, CHEN K, LI G, ZHOU L, ZHENG D, TU L, DONG XD. MicroRNA-206: effective inhibition of gastric cancer progression through the c-Met pathway. *PLoS One* 2015; 10: e0128751.